

An approximation of tribological behavior of $Ti_{1-x}Al_xN$ coatings against animal bone in Ringer's solution

A. Esguerra-Arce^a, N. A. Arteaga^a, C. Amaya^b, L. Ipaz^a, N. Alba de Sánchez^c, and Y. Aguilar^a

^aGrupo de investigación en Tribología-Polímeros-Metalurgia de Polvos y Residuos Sólidos, TPMR, Universidad del Valle, Calle 13 No. 100-00, Cali, Colombia, e-mail: adriana.esguerra.arce@gmail.com

^bGrupo de investigación en Desarrollo de Materiales y Productos, GIDEMP, Centro ASTIN, SENA, Calle 52 No.2 Bis-15, Cali, Colombia,

^cGrupo de investigación Ciencia e Ingeniería de Materiales, GCIM, Universidad Autónoma de Occidente, Calle 25 No.115-85, Cali, Colombia.

Received 22 November 2013; accepted 18 March 2014

Due to their excellent properties, Ti-Al-N coatings have become attractive for biomedical applications. In this paper, friction and wear properties of $Ti_{1-x}Al_xN$ films having various aluminum contents, x , have been studied. Adhesion was measured by the scratch test technique; friction was carried out by a pin-on-disk tribometer using an animal bone-pin as counterpart and Ringer's solution as simulated body fluid; and wear mechanisms were identified by SEM and EDS. It was found that the coating with $x = 0.41$ exhibited the highest COF, conserves its integrity as a coating, and causes the lowest wear on the bone in Ringer's solution.

Keywords: Sliding wear; PVD coatings; corrosion wear; biological aspects

PACS: 81.15.-z; 81.40.PQ

1. Introduction

Several kinds of alloys are available for biomedical applications based on titanium, nickel, aluminum, vanadium, chromium, zirconium, etc., approved by ASTM. However, some disadvantages are encountered with these alloys, because they mechanically destroy the normal bone with which they come in contact, causing allergy and inflammation due to abrasive particles and leached toxic ions [1]. Taking into account that the surface properties govern the material performance in this kind of applications, the modification of the surface of biomedical alloys to improve tribological properties could be considered as a solution. Ti-Al-N coatings seem to be an excellent material for this field, due to its excellent *in vivo* [2] and *in vitro* [3] biocompatibility, desirable electrochemical properties in simulated body fluids [2,4] and good mechanical behavior [5].

Considering that the application of this coating onto the surface of implants fixtures needs further investigation, the purpose of this work is to study the effect of atomic aluminum content, x , in $Ti_{1-x}Al_xN$ coatings deposited by reactive magnetron co-sputtering, in the tribological properties, such as friction coefficient and wear mechanisms, when submitted to conditions close to those found in the human body, using Ringer's solution and animal bone as counterpart. This research seeks to study the viability of using these coatings in orthopedic applications, by relating the tribological performance with mechanical properties and adhesion of the coatings.

2. Materials and Methods

$Ti_{1-x}Al_xN$ films were deposited on Si (100) and AISI 304ss substrates by reactive magnetron co-sputtering at 250°C with

high purity titanium and aluminum targets. The substrates were ultrasonically cleaned in isopropyl alcohol and acetone sequentially and then dried in air jet before being placed into the vacuum chamber. The base pressure in the chamber was 2.1×10^{-4} mBar and the working pressure was set at 2.0×10^{-2} mBar during deposition. A titanium buffer-layer was deposited on the substrate in presence of Ar. The power applied to the Ti target was 400 W. Nitrogen gas was injected afterwards (Ar flow: 50 sccm; N_2 flow: 3.7 sccm) into the deposition chamber and the power applied to the Al target (10.16 cm in diameter) was varied in 200, 250 and 350 W for reactive deposition of TiAlN. Due to the variation in aluminum sputter yielding, the deposition time varied in 2.0, 1.5 and 1.2 hours, respectively. The substrates were rotated at a speed of 21 rev/min in order to obtain homogeneous film composition and the r. f. bias voltage at the substrate was put at -20 V.

EDS analysis was performed to determine the contents of Ti, Al and N. An X-ray diffraction (XRD) study was carried out using an X'pert HighScore Plus diffractometer with $Cu-K\alpha$ radiation ($\alpha = 1.5406 \text{ \AA}$) at grazing angle of 0.5° . The morphological characterization of the coatings (grain size) was obtained using an atomic force microscope (AFM) from Asylum Research MFP-3D® using a cantilever silicon tip in non-contact mode and calculated by a Scanning Probe Image Processor (SPIP®) which has the standard program for processing and presenting AFM data. Thickness was evaluated by SEM (JEOL JSM-649 OLV).

A cortical bone specimen was prepared from a pig humerus obtained from a local market. The bone was immersed in water at 100°C for 2 h to remove soft tissue attached to the bone. In order to prevent changes in the bone's mechanical properties, the humerus was never allowed to touch the heat source while being slowly heated. After this

process, the remnant soft tissue attached to the bone was mechanically removed by hand and then the bone was cleaned, dried in ambient air and mechanized to spherical form.

Adherence was studied by using a Scratch Test Microtest MTR2 system, with a 6 mm scratch length and a raising load of 0–90 N. To identify the different adherence failures an optical microscope was used. To identify the different adherence failures, the adhesion properties of coatings can be analyzed by the following two terms, L_{c1} , the lower critical load defined as the load where the first cracks occurred (cohesive failure) and the L_{c2} , detachment and separation of a coating from the substrate with cracking and de-bonding at the coating-substrate interface (adhesion failure) [6].

Each sample was indented 24 times using a Berkovich

pyramidal indenter, varying the maximum load applied from 479.6 to 5995.8 μN (10 seconds of loading and 10 seconds of unloading). The elastic properties were calculated for each indent and the reduced modulus was calculated by the Pharr–Oliver relationship [7].

To evaluate the tribological properties of the $Ti_{1-x}Al_xN$ coatings, sliding wear tests were carried out by using a MicroTest pin-on-disc tribometer (two replicates). The tests were performed at a normal load of 10 N using an animal-bone ball with 6 mm in diameter, as the wear counterpart, and Ringer's solution as simulated body fluid. The sliding linear speed and total sliding distance were set at 8 mm/s and 400 m, respectively. The wear tracks were studied by EDS and SEM (JEOL JSM-649 OLV).

TABLE I. Characteristics of the samples.

Sample	Hardness (GPa)	Young's Modulus (GPa)	Roughness (nm)	Grain diameter (nm)	Thickness (nm)
304ss	5.3 ± 0.7	234 ± 12	37.5 ± 2		
$x = 0.24$	28.5 ± 0.3	260 ± 13	92.5 ± 5	85 ± 4	566
$x = 0.41$	29.6 ± 0.4	304 ± 15	35.0 ± 2	53 ± 3	557
$x = 0.60$	22.6 ± 0.5	278 ± 13	71.3 ± 4	80 ± 4	883
Bone	6.0 ± 1.0	18.8 ± 2			

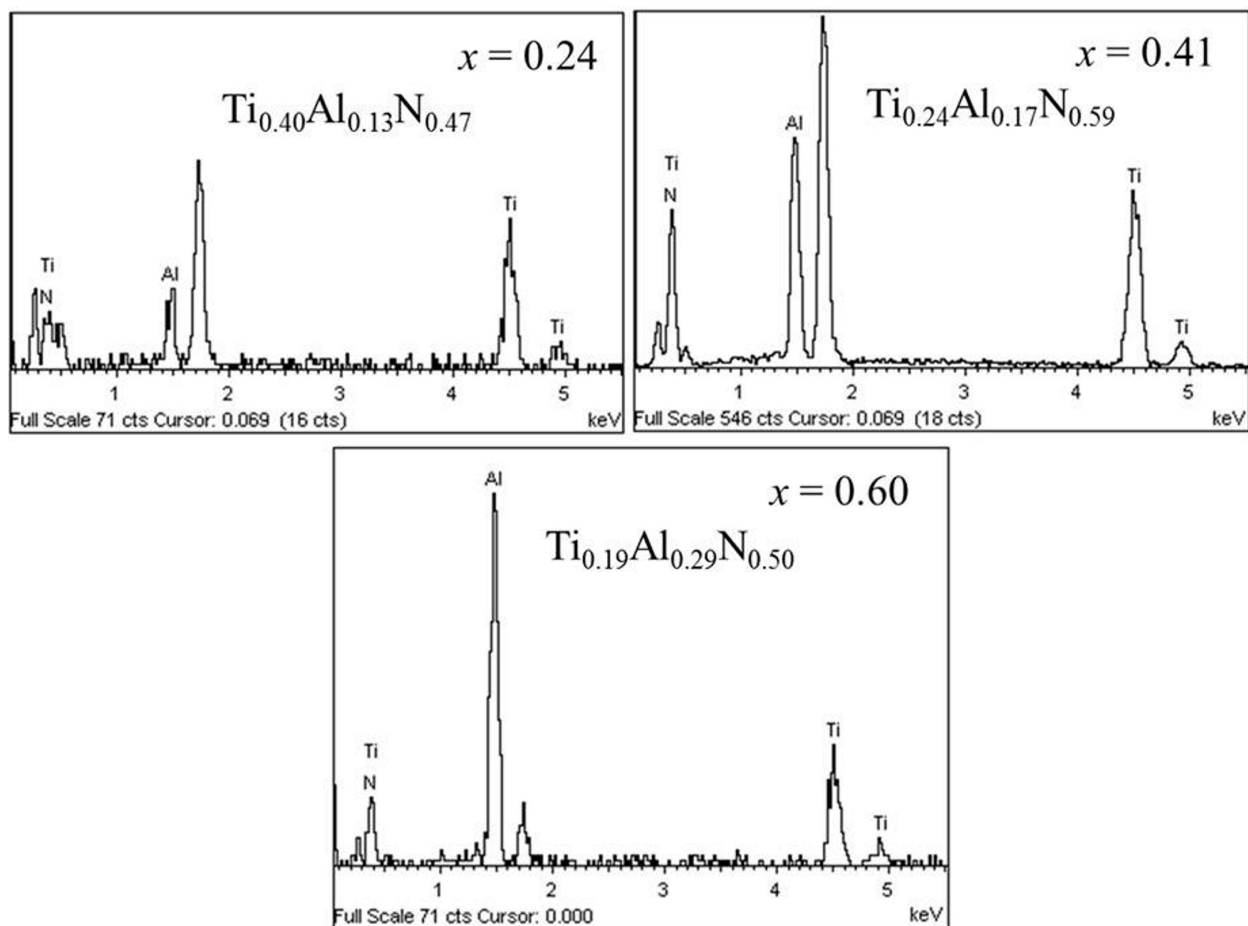


FIGURE 1. EDS spectra of the coatings.

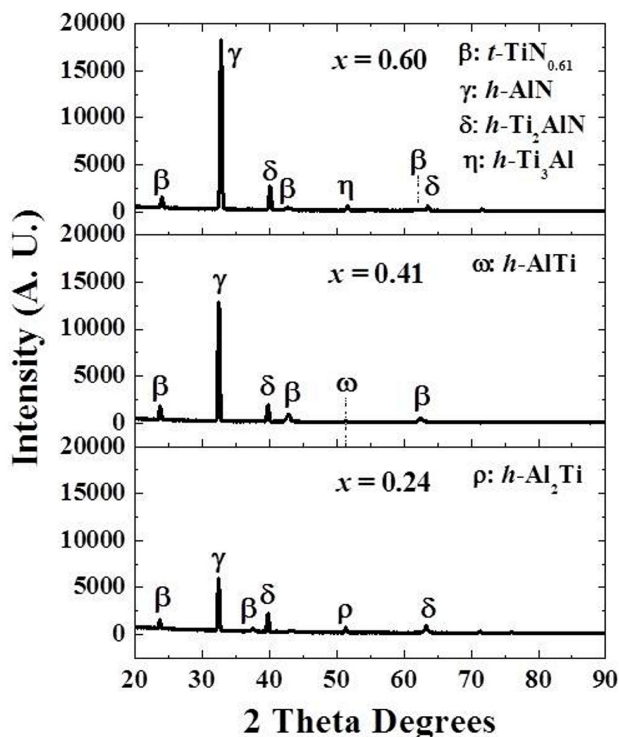


FIGURE 2. XRD diffractograms of the coatings.

3. Results

3.1. Chemical composition, microstructure, thickness and mechanical properties

Figure 1 shows the EDS spectra and chemical composition of the coatings. The chemical composition strongly depended on the power applied to the aluminum target. The value of x will be used to show the Al content in $Ti_{1-x}Al_xN$ films ($x = Al/(Ti+Al)$). The XRD diffractograms of the samples are depicted in Fig. 2, which shows that coatings generally contain B4-Wurtzite AlN, hexagonal Ti_2AlN and tetragonal $TiN_{0.61}$. Besides these phases, the presence of intermetallic phases is observed: Ti_3Al for coatings with $x = 0.24$, $TiAl$ for coatings with $x = 0.41$ and $TiAl_2$ for coatings with $x = 0.60$. The presence of the B4-Wurtzite AlN phase is incremented by adding of aluminum to the coatings. The roughness, grain diameter, thickness, hardness and Young's Modulus of the coatings and substrate are shown in Table I.

3.2. Adhesion behavior

Figure 3 shows the optical micrographs of the surface tracks. For films with $x = 0.24$ and 0.41 , it was observed that coating buckles ahead of the tip, producing irregularly-spaced arcs opening away from the direction of the scratching. This behavior is common in thinner coatings. For the film with $x = 0.60$ a change in the crack damage is observed, feature seen in the failure: the buckling cracks change to buckling spallation, which is similar to buckling, but with wide arc-

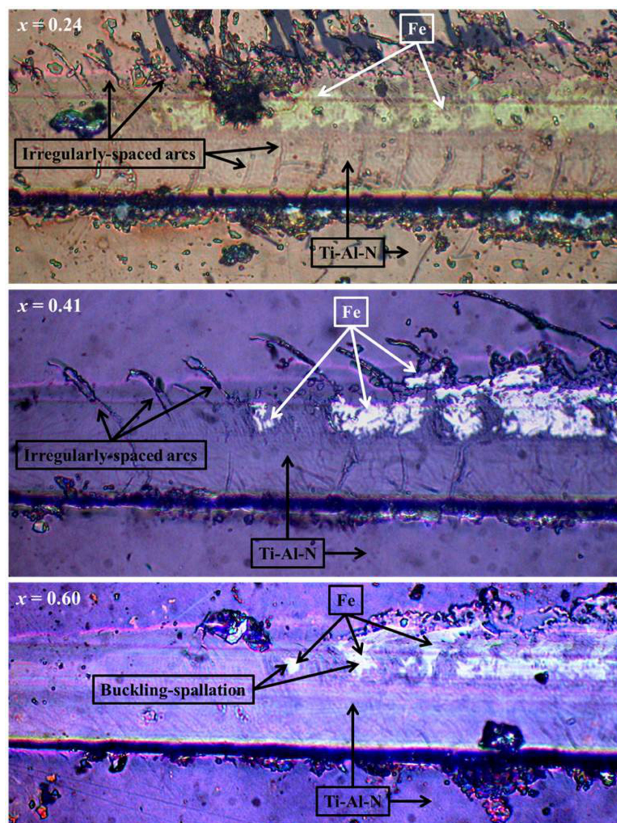


FIGURE 3. Optical micrographs of scratch tracks on $Ti_{1-x}Al_xN$ films.

shaped patches missing [6]. Spalling is a result of total detachment of the coating from the substrate and flaking off, while conformal and tensile cracking takes place when the coating remains fully adhered [8].

The critical loads were obtained from the optical images and stylus drag coefficient *versus* distance graphics. The L_{c2} for the different coatings were in the range of 3.8-4.2 N. The lowest value is attributed to the coatings with $x = 0.60$ and the highest value is attributed to the coatings with $x = 0.41$. It was noted that the adhesive critical load increased when the aluminum content reached 0.41, whereas this value decreased when the aluminum contents reached 0.60. This behavior agrees with that reported by Shum *et al* [9] and Anderbouhr *et al* [10].

3.3. Friction

A comparison of the coated specimens regarding the relationship between the friction coefficient and the travel distance is shown in Fig. 4. For all samples, except for replica 1 of the coating with $x = 0.24$, the friction coefficient rose from zero to a determined value and then stabilized for the rest of the test, a steady state. This value is 0.38 ± 0.02 , 0.44 ± 0.02 and 0.37 ± 0.03 for coatings with $x = 0.24$, 0.41 and 0.60 , respectively.

Figure 5 shows the behavior of average coefficient of friction with atomic aluminum content in coatings, x . It is shown

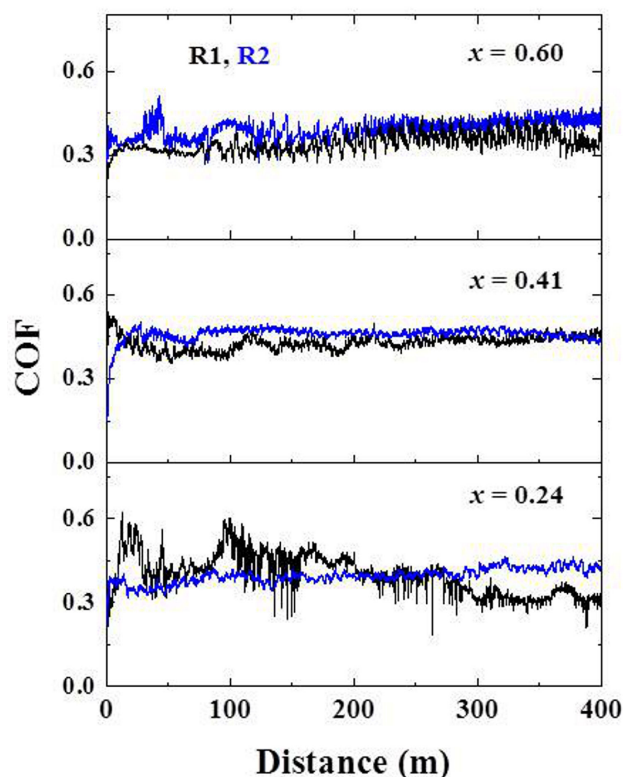


FIGURE 4. Comparison of the coated specimens regarding the relationship between the friction coefficient (COF) and the travel distance.

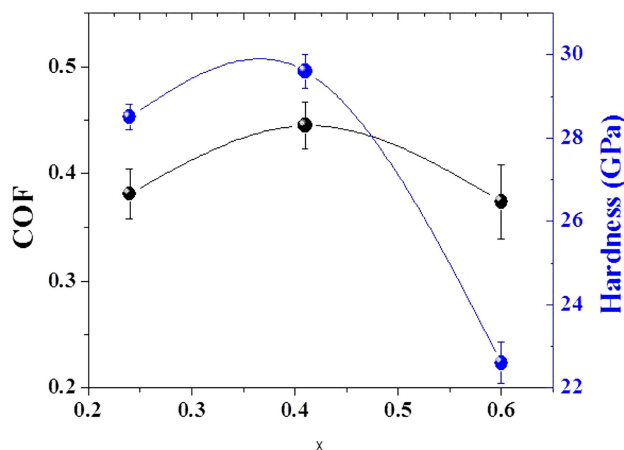


FIGURE 5. Comparison of COF and coating hardness values for each sample.

that the coating with $x = 0.41$ exhibits the highest friction coefficient, likely related to the highest hardness value exhibited by this coating, because a correlation between friction coefficient values and the hardness of the discs can be seen: films with higher hardness values exhibit higher friction with the bone in Ringer's solution.

Considering that the friction coefficient is an important value in biomaterials design, given that the friction coefficient affects the relative micromotion in the biomaterial-bone interface (for example, increasing the friction coefficient causes

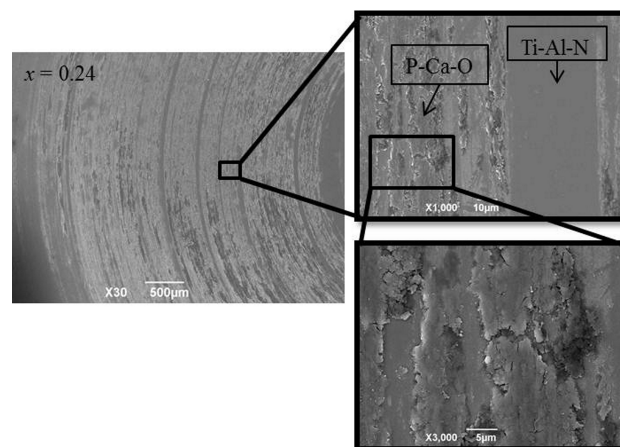


FIGURE 6. Wear mechanism of the coating with $x = 0.24$.

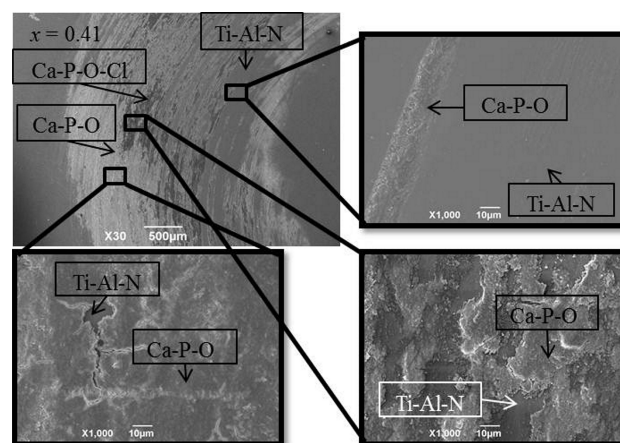


FIGURE 7. Wear mechanism of the coating with $x = 0.41$.

the peak micromotion between cup-pelvis pair to be reduced [11]), the coating with $x = 0.41$ would be the more appropriate for this application.

3.4. Wear

SEM inspection of the scars generated using the bone counterpart was made to verify the actual predominant wear mode. For the coatings with $x = 0.24$ (Fig. 6) and 0.41 (Fig. 7) the adhesive wear mechanism is observed. EDS analysis, which showed the presence of phosphorus, calcium and oxygen in this adhered film, confirmed that this is a bone layer adhered to the coatings surface. Also it was observed, by the EDS analysis, that coatings conserve their integrity and do not suffer detachment, because it were not observed the presence of iron or chromium atoms at the surface, but titanium, aluminum and nitrogen were observed, indicating the steel was covered and protected by the Ti-Al-N coating.

On the contrary, coatings with $x = 0.60$ (Fig. 8) exhibited detachment, as can be seen in SEM micrographs. The latter is evidenced in EDS analysis of the surface, given that the surface exhibit the presence of iron and chromium, principal components of the stainless steel. Besides this, the surface

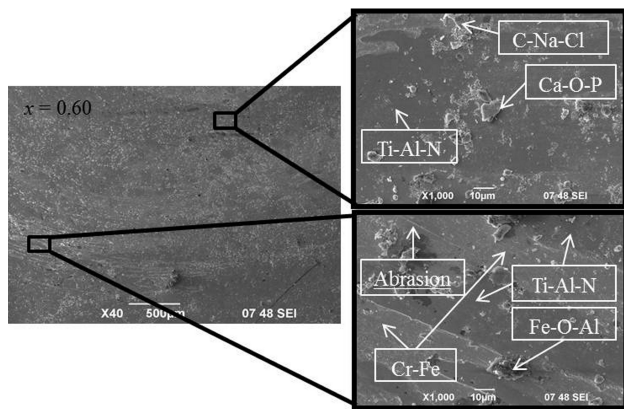


FIGURE 8. Wear mechanism of the coating with $x = 0.60$.

also exhibits the presence of oxidized iron particles, produced by the interaction of the steel surface with the simulated body fluid. The exposition of the AISI 304ss substrate to the simulated body fluid also caused abrasive wear of the substrate by the bone and Ti-Al-N debris particles. This behavior is probably related to the adhesion of the coatings, because the coating with $x = 0.60$ exhibited the lower adherence resistance of the coating to the substrate, and to the electrochemical properties of the coatings in simulated body fluid (unpublished results), because coatings with $x = 0.60$ exhibit lower values

of corrosion current density and polarization resistance than AISI 304 ss, which does not happen in other coatings.

Regarding the counterpart, bone pins, it was observed that the counterparts of coatings with $x = 0.60$ exhibit eight times more wear, $(3.99 \pm 0.57) \times 10^{-3} \text{ mm}^3/\text{N} \times \text{m}$, than the counterpart of other coatings, $(4.71 \pm 0.11) \times 10^{-4}$ and $(5.02 \pm 1.19) \times 10^{-4} \text{ mm}^3/\text{N} \times \text{m}$, via coatings with $x = 0.24$ and 0.41 , respectively. This behavior is probably related to the detachment exhibited by the coating with $x = 0.60$, which produced debris cause the more pronounced wear of the bone.

4. Conclusions

From this study it may be concluded that $\text{Ti}_{1-x}\text{Al}_x\text{N}$ coatings with $x = 0.24$ and 0.41 could be used to protect AISI 304 stainless steel from tribological wear in Ringer's solution, because they conserve their integrity as coating and causes the lesser wear to the bone, which could suggest that these coatings could be used in biomedical applications. Taking into account the friction coefficient, coating with $x = 0.41$ should be the best option. On the contrary, the coating with $x = 0.60$ exhibited detachment, exposing the substrate and causing abrasion wear. Moreover, this counterpart causes the greatest wear on the bone.

1. G. Schmalz and P. Garphammer, *Dent. Mater.* **18** (2002) 396
2. K.H. Chung, G.T. Liu, J.G. Duh and J.H. Wang, *Surf. Coat. Technol.* **188** (2004) 745
3. Chia-Chi Chien, Kuan-Ting Liu, Jenq-Gong Duh, Kuo-Wei Chang and Kwok-Hung Chung, *Dent. Mater.* **24** (2008) 986
4. B. Subramanian, R. Ananthakumar and M. Jayachandran, *Vacuum* **85** (2010) 601
5. Z. Liu, P. Shum and Y. Shen, *Thin Solid Films* **468** (2004) 161
6. ASTM C1624-05, West Conshohocken, PA, *American Society for Testing and Materials*, (2010)
7. W.C. Oliver, G. M. Pharr, *Journal of Materials Research* **7** (1992) 1564
8. K. Holmberg and A. Matthews, *Tribology and Interface Engineering Series*, 2nd ed. (Elsevier, Vol. 56, 2009), pp. 128.
9. P.W. Shum, W.C. Tam, K.Y. Li, Z.F. Zhou, Y.G. Shen, *Wear* **257** (2004) 1030–1040
10. S. Anderbouhr, V. Ghetta, E. Blanquet, C. Chabrol, F. Schuster, C. Bernard, R. Madar, *Surf. Coat. Technol.* **115** (1999) 103–110
11. J. T. Hsu, C. H. Chang, H. L. Huang, M. E. Zobitz, W. P. Chen, K. A. Lai, K. N. An, *Med. Eng. Phys.* **29** (2007) 1089–1095